Parametric Covariance Propagation in the non-linear diffusive Burgers equation

O. Pannekoucke[1,2], M. Bocquet[3], R. Menard[4]

[1]INPT-ENM, CNRM UMR 3589, Météo-France/CNRS, Toulouse, France [2]CERFACS, Toulouse, France
[3] CEREA, joint lab École des Ponts ParisTech and EdF R&D, Université Paris-Est, France
[4]ARQI/Air Quality Research Division, Environment and Climate Change Canada, Dorval (Québec), Canada

1. Context

Remind on covariance propagation

If a system is governed by a nonlinear dynamics $\frac{d\boldsymbol{u}}{dt} = \mathcal{M}(\boldsymbol{u})$ where $\boldsymbol{u} \in \mathbb{R}^n$, then the time evolution of a perturbation, along a particular nonlinear solution, is given by the tangent linear (TL) equations

$$\frac{d\varepsilon}{dt} = \mathbf{M}\varepsilon. \tag{1}$$

If the initial perturbation, ε_0, is a random centered Gaussian vector of covariance matrix $\mathbf{B}_0$, $\varepsilon_0 \sim \mathcal{N}(0, \mathbf{B}_0)$, then the perturbation at time t, ε_t, is also Gaussian with covariance matrix

$$\mathbf{B}_t = \mathbf{M}_t \mathbf{B}_0 \mathbf{M}_t^T, \tag{2}$$

where $\mathbf{M}_t$ is the propagator associated with Eq.(1).

Problematic of the covariance dynamics and the parametric formulation

Equation (2) is the Kalman fitler forecast equation, whose implementation in large system is beyond the computer capacity since it requires to n time integration of the TL equation (and its adjoint).

[Pannekoucke et al., 2016] have explored a simplicitation of this covariance matrix dynamics that is based on a parametric formulation of the covariances and is applied for the particular linear advection-diffusion equation. In this contribution, we extend this idea in the nonlinear setting: the diffusive nonlinear Burgers equation.

2. Parametric covariance dynamics for the Burgers equation

The diffusive nonlinear Burgers dynamics

Here, we consider the dynamics associated with the Burgers equation

$$\partial_t u + u\partial_x u = \kappa \partial_x^2 u. \tag{3}$$

For a particular initial condition $u(x,0) = u_0(x)$, there exist a unique solution of Eq.(3), denoted u.

Reynolds décomposition $u = \overline{u} + \varepsilon$ can be introduced to describe the time evolution of a mean state and perturbation around it. These dynamics are described by the coupled system

$$\begin{cases} (a)\ \partial_t \overline{u} + \overline{u}\partial_x \overline{u} = \kappa\partial_x^2 \overline{u} - \overline{\varepsilon\partial_x\varepsilon}, \\ (b)\ \partial_t \varepsilon + \overline{u}\partial_x \varepsilon = -\varepsilon\partial_x \overline{u} + \overline{\varepsilon\partial_x\varepsilon} + \kappa\partial_x^2\varepsilon - \varepsilon\partial_x\varepsilon. \end{cases} \tag{4}$$

This makes appear perturbation-mean flow interaction, where the contribution $-\overline{\varepsilon\partial_x\varepsilon}$ in the dynamics of $\overline{u}$, Eq.(4-a), is the shift of the mean state due to the perturbation activity. In return, $\overline{\varepsilon\partial_x\varepsilon}$ in Eq.(4-b), describe the intertial shift due to the change of the average. In particular, this last contribution does not affect the statistical properties of the perturbations ε, while it is crucial to the dynamics of $\overline{u}$.

In case of small magnitude perturbation ε, the Reynolds equations Eq.(4) are simplfied into the tangent linear dynamics

$$\begin{cases} \partial_t \overline{u} + \overline{u}\partial_x \overline{u} = \kappa\partial_x^2 \overline{u} - \overline{\varepsilon\partial_x\varepsilon}, \\ \partial_t \varepsilon + \overline{u}\partial_x \varepsilon = -\varepsilon\partial_x \overline{u} + \overline{\varepsilon\partial_x\varepsilon} + \kappa\partial_x^2\varepsilon. \end{cases} \tag{5}$$

Illustration of error time propagation

Thereafter, we consider the Burgers dynamics on a periodic domain of size $L = 1000$km, discretized in 241 grid points. The initial covariance matrix $\mathbf{B}_0$ is of constant variance and homogeneous Gaussian correlation functions. The standard deviation σ^ε can take two values, $\sigma^\varepsilon = 1\% U_{max}$ and $\sigma^\varepsilon = 10\% U_{max}$, in order to tackle the limits of the TL dynamics. The length-scale $L_h = \sqrt{2\nu}$ is set to $2\% L$. The time integration of two perturbations with amplitude $\sigma^\varepsilon = 1\% U_{max}$ (a) and $\sigma^\varepsilon = 10\% U_{max}$ (b), is shown in Fig.(1).

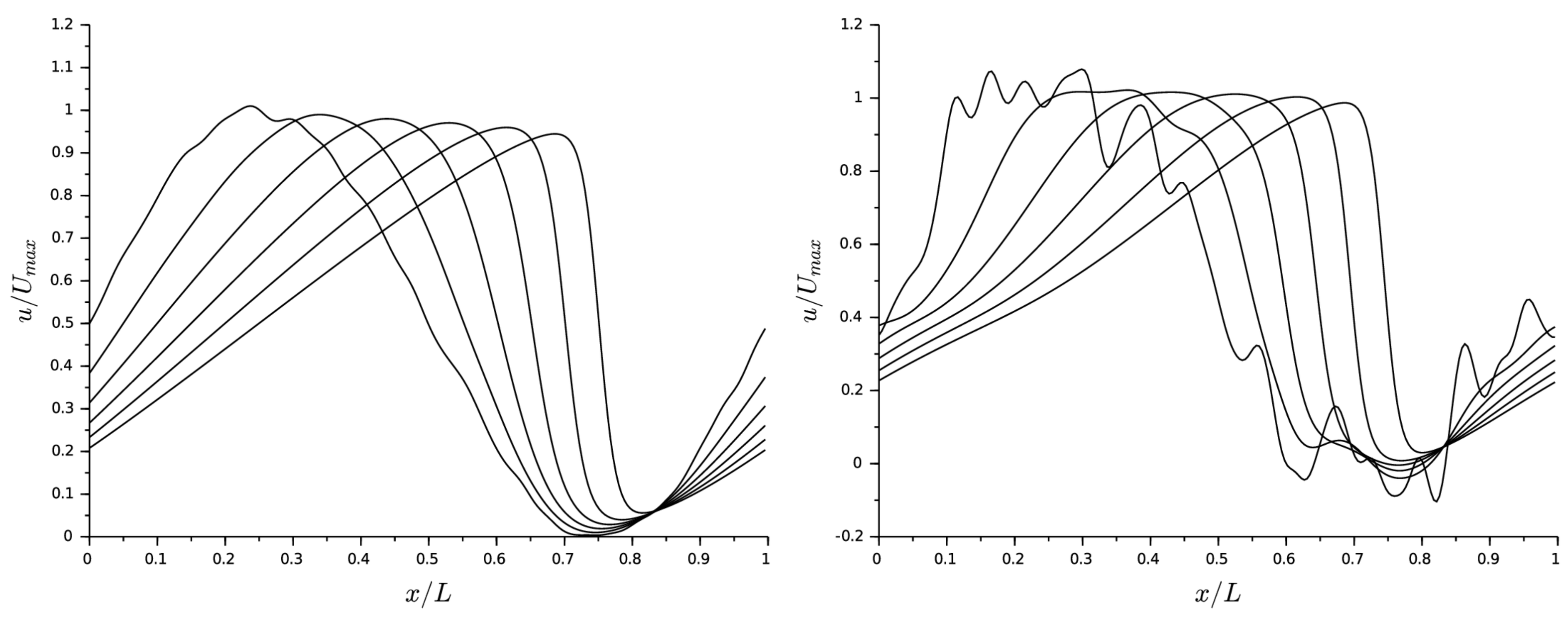

(a) (b)

Figure: 1- Illustration of a perturbed evolution for intial perturbation standard deviation magnitude of $\sigma^\varepsilon = 1\% U_{max}$ (a) and $\sigma^\varepsilon = 10\% U_{max}$ (b), for the time $t = \{0, 0.2, 0.4, 0.6, 1\}$UT, where the unit time is UT=6h.

Parametric covariance modelling

In the parametric covariance modelling introduced in [Pannekoucke et al., 2016] only the variance field $V_{\boldsymbol{x}}$ and the local metric field are retained to feature the covariance. The variance field corresponds to the diagonal of the covariance matrix $\mathbf{B}$, $V_{\boldsymbol{x}} = \mathbf{B}(\boldsymbol{x}, \boldsymbol{x})$, while the local metric field $\boldsymbol{g}_{\boldsymbol{x}}$, associated with the correlation functions $\rho(\boldsymbol{x}, \boldsymbol{y}) = \mathbf{B}(\boldsymbol{x}, \boldsymbol{y})/\sqrt{V_{\boldsymbol{x}} V_{\boldsymbol{y}}}$, is deduced from the second order Taylor expansion

$$\rho(\boldsymbol{x}, \boldsymbol{x} + \delta\boldsymbol{x}) \underset{\delta\boldsymbol{x}=0}{=} 1 - \frac{1}{2}||\delta\boldsymbol{x}||^2_{\boldsymbol{g}_{\boldsymbol{x}}} + o(||\delta\boldsymbol{x}||^2), \tag{6}$$

where $||\mathbf{x}||^2_{\mathbf{E}} = \mathbf{x}^T\mathbf{E}\mathbf{x}$. The construction of a covariance matrix from the variance field and from the local metric field can be achieved considering the covariance model based on the diffusion equation [Weaver and Courtier, 2001]. In this case, the local diffusion tensor $\boldsymbol{\nu}_{\boldsymbol{x}}$ is related to the local metric tensor [Pannekoucke and Massart, 2008] following

$$\boldsymbol{\nu}_{\boldsymbol{x}} = \frac{1}{2}\boldsymbol{g}_{\boldsymbol{x}}^{-1}. \tag{7}$$

Parametric covariance forecast

Following a similar derivation to [Cohn, 1993], it is *straightforward* to verify that the variance and the diffusion tensor are governed by the variance-diffusion coupled dynamics

$$\begin{cases} (a)\ \partial_t \overline{u} + \overline{u}\partial_x \overline{u} &= \kappa\partial_x^2\overline{u} - \frac{1}{2}\partial_x V, \\ (b)\ \partial_t V + \overline{u}\partial_x V &= -2(\partial_x\overline{u})V + \kappa\partial_x^2 V_x - \frac{\kappa}{2}\frac{1}{V_x}(\partial_x V_x)^2 - \frac{\kappa}{\nu_x}V_x, \\ (c)\ \partial_t\nu_x + \overline{u}\partial_x\nu_x &= 2(\partial_x\overline{u})\nu_x + 2\kappa - 2\frac{\kappa}{V_x}\partial_x^2 V_x\,\nu_x + 2\frac{\kappa}{V_x^2}(\partial_x V_x)^2\nu_x + 2\kappa\frac{1}{V_x}\partial_x V_x\partial_x\nu_x + \kappa\partial_x^2\nu_x \\ & \quad -2\kappa\frac{1}{\nu_x}(\partial_x\nu_x)^2. \end{cases} \tag{8}$$

Compared with Eq.(2), the parametric dynamics simplifies the covariance propagation by only forecasting the variance and the local metric tensor fields, that requires only two additionnal fields in the preset forecast integration. With this approach, a single time integration replaces the n tangent linear integration of Eq.(2).

3. Numerical experience

The parametric forecast is based on the time integration of the non-linear coupled system Eq.(8), whose numerical cost is of the order of a non-linear time integration of the Burgers equation. In this one-dimensional case, only two scalar fields are forecasted: the variance V and the local diffusion tensor ν (reduced to a single field for this framework).

Ensemble validation of the parametric dynamics

The variance and the length-scale field are reproduced in Fig.(2) and Fig.(3), which compare the diagnosis resulting from the nonlinear forecast of a large ensemble of $N_e = 1600$ members (continuous line) with the parametric solution provided by the equation Eq.(8). It appears that the ensemble statistics are accurately predict from the analytical formulation when initial error standard deviation magnitude is small ($\sigma^\varepsilon = 1\% U_{max}$) but when the non-linear effect are larger ($\sigma^\varepsilon = 10\% U_{max}$), then the skill of the analytical dynamics is lower.

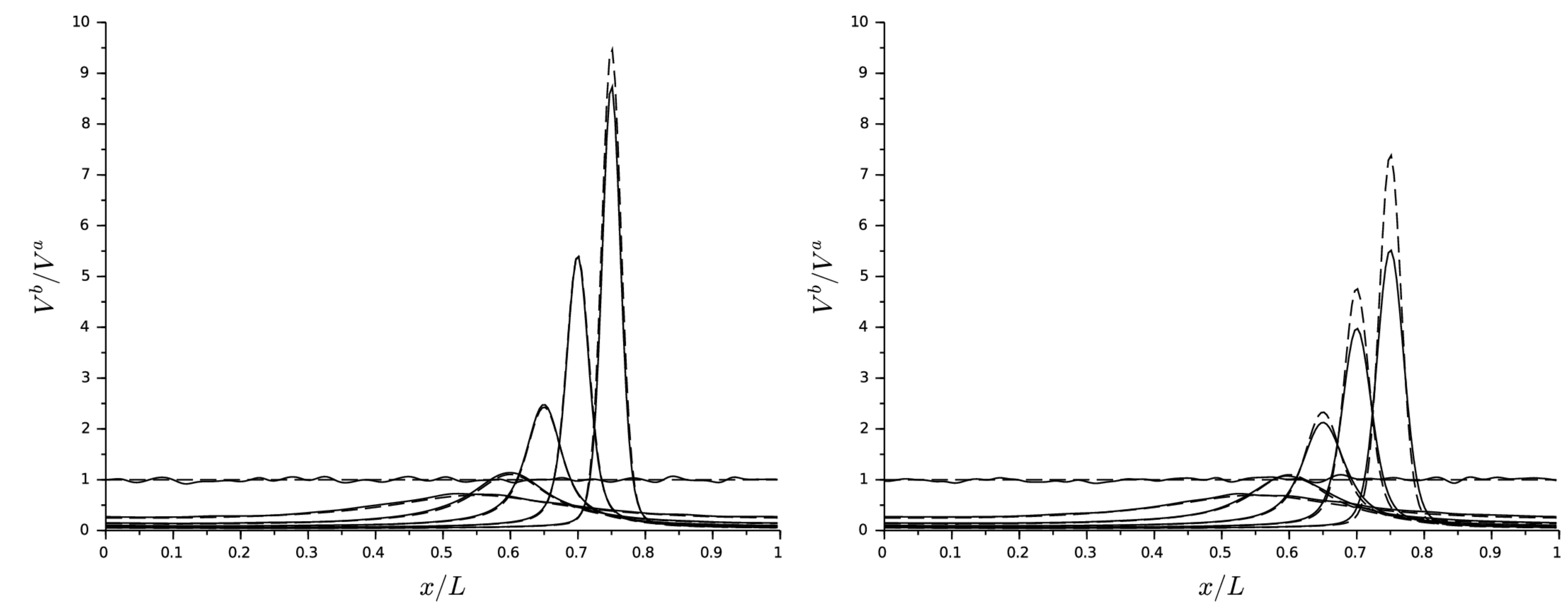

(a) (b)

Figure: 2- Analytical (dashed line) vs. numerical (continous line) variance fields for intial perturbation of standard deviation magnitude $\sigma^\varepsilon = 1\% U_{max}$ (a) – tangent linear dyanmics – and $\sigma^\varepsilon = 10\% U_{max}$ (b) – weakly non-linear dynamics.

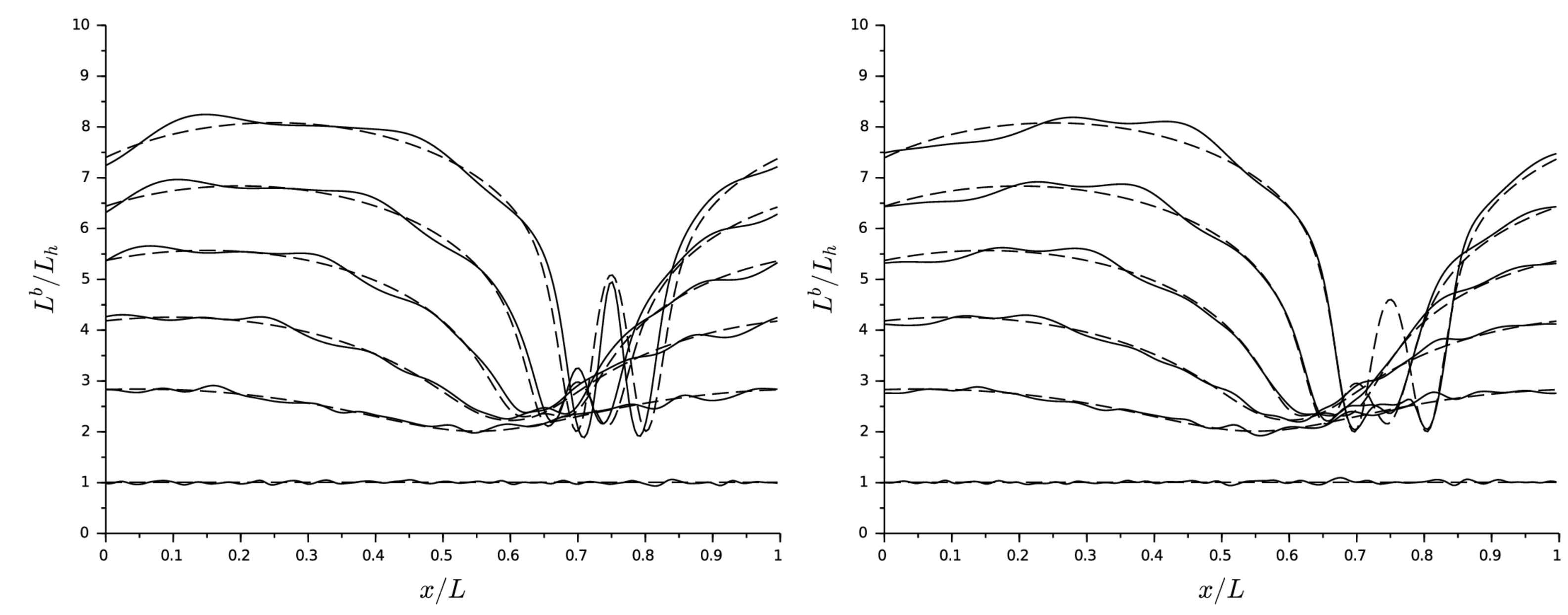

(a) (b)

Figure: 3- Analytical (dashed line) vs. numerical (continous line) length-scale field for intial perturbation of standard deviation magnitude $\sigma^\varepsilon = 1\% U_{max}$ (a) – tangent linear dyanmics – and $\sigma^\varepsilon = 10\% U_{max}$ (b) – weakly non-linear dynamics.

Limitation due to the nonlinear dynamics and beyond the TL setting

In order to understand more precisely the role of the nonlinear terms $\varepsilon\partial_x\varepsilon$ on the error dynamics, a second ensemble validation has been conducted, represented in Fig.4. This figure reproduces, at the final time, the variance and the length-scale fields $L_{\boldsymbol{x}} = \sqrt{2\nu_{\boldsymbol{x}}}$ computed with the parametric statistics (dashed line), diagnosed from a large non-linear ensemble (continuous line) shown in Fig.2-3. Then it represents the statistics computed from an ensemble of forecast of the TL dynamics Eq.(5) (small dashed line), and using the Reynolds equations Eq.(4) (dash-dotted line).

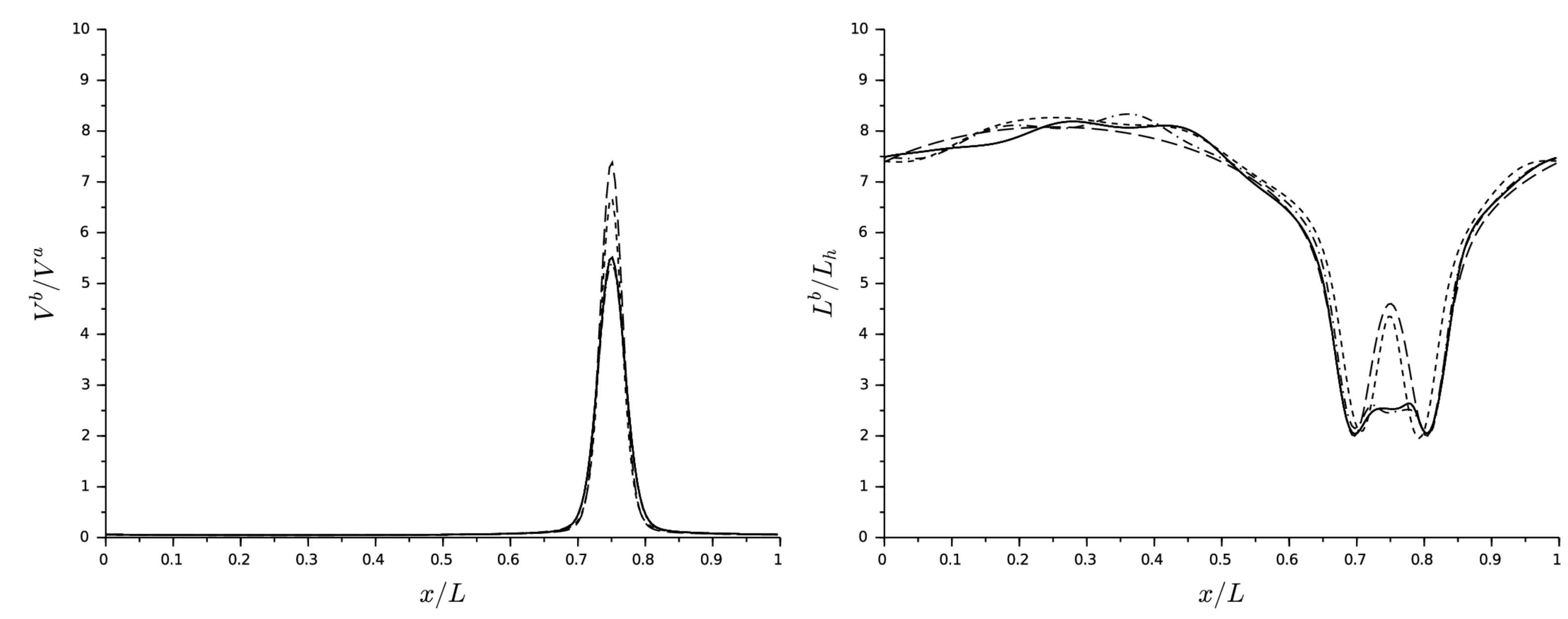

(a) (b)

Figure: 4- Verification of the parametric forecast of the variance (a) and the correlation length-scale (b) at the final time and for an initial perturbation standard deviation magnitude of $10\% U_{max}$. The diagnosed result for the non-linear ensemble is in continuous line, the theoretical forecsated statistics are in dashed line, the ensemble without (with) second order term $\varepsilon\partial_x\varepsilon$ is in small dashed line (dash-dotted line).

4. Conclusions and Perspectives

In this contribution, we have presented the derivation of the parametric covariance forecast for the diffusive nonlinear Burgers equation. The parametric formulation relies on the forecast of the variance and the local metric tensor. A full covariance matrix can then be deduced from the covariance model based on the diffusion equation, where the local metric tensor is then used to specify to the local diffusion. This parametric formulation has been compared with the nonlinear propagation of a large ensemble from which the reference variance and local metric fields have been diagnosed. The results are that when the tangent linear assumption is verified the parametric formulation is able to reproduce the true statistics. When the magnitude of the error is large, we have shown that the parametric formulation was not able to reproduce the reference, and that this limitations was due the the nonlinearity.

This contribution illustrates the feasibility of the parametric formulation in the nonlinear setting where extension toward geophysical application should be the next step.

5. References

Cohn, S. (1993).
Dynamics of short-term univariate forecast error covariances.
Monthly Weather Review, 121(11):3123–3149.

Pannekoucke, O. and Massart, S. (2008).
Estimation of the local diffusion tensor and normalization for heterogeneous correlation modelling using a diffusion equation.
Q. J. R. Meteorol. Soc., 134:1425–1438.

Pannekoucke, O., Ricci, S., Barthelemy, S., Menard, R., and Thual, O. (2016).
Parametric kalman filter for chemical transport model.
Tellus, pages XX–XX.

Weaver, A. and Courtier, P. (2001).
Correlation modelling on the sphere using a generalized diffusion equation (tech. memo. ecmwf, num. 306).
Quarterly Journal Royal Meteorological Society, 127:1815–1846.